A Novel Sliding Mode Fuzzy Control based on SVM for Electric Vehicles Propulsion System

Allaoua Boumediène[1] and **Laoufi Abdellah**[2], Non-members

ABSTRACT

This paper presents a new sliding mode fuzzy control (SMFC) scheme for torque control of induction motors of the electric vehicles propulsion system. The control principle is based on sliding mode fuzzy control combined with space vector modulation (SVM) technique. The sliding mode fuzzy control contributes to the robustness of induction motor wheel drives of the electric vehicle propulsion system, and the space vector modulation improves the torque, flux, and current steady-state performance by reducing the ripple. The Lyapunov direct method reinforced with fuzzy logic is used to ensure the reaching and sustaining of sliding mode and stability of the control system. The performance of the proposed system is compared with those of conventional sliding mode controller and classical PI controller. Finally, computer simulation results verify the validity of the proposed method and show that the proposed control scheme provides robust dynamic characteristics with low torque ripple.

Keywords: Control Robustness, Electric Vehicle Propulsion System, Low Torque Ripple, Sliding Mode Fuzzy Control, Space Vector Modulation.

1. INTRODUCTION

The application of induction motors (IM) in traction systems, including electric vehicles, requires comparison of available drives for traction. The IM is the best choice for electric vehicle driving motor, since it has simple structure, reliable operation, high efficiency and large power density[1, 2, 3].The IM is widely used in industry applications, mainly due to its rigidness, maintenance-free operation, and relatively low cost. In contrast to the commutation DC motor, it can be used in aggressive or volatile environments since there are no risks of corrosion or sparks. However, induction motors constitute a theoretically challenging control problem since the dynamical system is nonlinear, the electric rotor variables are not measurable, and the physical parameters are most often imprecisely known. The control of the IM has attracted much attention in the past few decades; especially the speed sensorless control of induction motors has been a popular area due to its low cost and strong robustness [4].

In the field of electric vehicle, the efficiency of the IM should be higher for lengthening the cruising distance. Meanwhile, the dynamic torque response should also be good. Classical PI controller is a simple method used in control of IM drives. However, the main drawbacks of PI controller are the sensitivity of performance to the system parameter variations and inadequate rejection of external disturbances and load changes [5, 6]. Sliding mode control (SMC) is a robust control since the high gain feedback control input suppresses the influence of the disturbances and uncertainties [7]. Due to its order reduction, good disturbance rejection, strong robustness, and simple implementation by means of power inverter, SMC has attracted much attention in the electric drive industry, and becomes one of the prospective control methodologies for IM wheel drives of the electric vehicles propulsion system [8].

Fuzzy logic control and SMC have been combined in a variety of ways for sliding surface design [9, 10]. These approaches can be classified into two categories. The first approach taken by many researchers is to use fuzzy logic control for the determination of the sliding surface movement of the classical SMC [10, 11]. A Takagi-Sugeno type fuzzy tuning algorithm is used for the movement of the sliding surface [6, 12, 13, 14]. The aim objective of the second approach is to determinate directly the sliding surface based on fuzzy logic, this method called sliding mode fuzzy control (SMFC).

SMC acts in a transient state to enhance the stability, while fuzzy technique functions in the steady state to reduce chattering. The Lyapunov direct method is used to ensure the reaching and sustaining of the sliding mode [15, 16, 17]. These SMC methods result in a good transient performance, sound disturbance rejection, and strong robustness in a control system. However, the chattering is a problem in SMC and causes the torque, flux, and current ripple in the systems.

With the development of microprocessors, the space vector modulation (SVM) technique has become one of the most important pulse width modulation (PWM) methods for voltage source inverter (VSI). It uses the space vector concept to compute the duty cycle of the switches. It simplifies the digital implementation of PWM modulations. An apti-

Manuscript received on October 21, 2011 ; revised on June 10, 2012.

[1,2] The authors are with Department of Technology, Faculty of the Sciences and Technology, BECHAR University, B.P 417 BECHAR (08000), ALGERIA., E-mail: elec_allaoua2bf@yahoo.fr and laoufi_ab@yahoo.fr

tude for easy digital implementation and wide linear modulation range for output line-to-line voltages are the notable features of SVM [18, 19, 20]. Thus SVM becomes a potential technique to reduce the ripple in the torque signal.

This paper presents a new sliding mode fuzzy controller for torque regulation of induction motor wheel drives of the electric vehicle propulsion system. This novel control method integrates the speed sensorless SMC with the SVM technique. It replaces the PWM component in the conventional SMFC with the SVM so that the torque ripple of induction motor wheel drives is effectively reduced while the robustness is ensured at the same time. In this new technique, the ripples of both torque and flux are reduced very remarkable, and switching frequency is maintained constant. Simulation results verify the validity of the proposed method.

2. SVM TECHNIQUES IN INDUCTION MOTOR DRIVES

The SVM technique is the more preferable scheme to the PWM voltage source inverter since it gives a large linear control range, less harmonic distortion, and fast transient response [19, 20]. A scheme of a three-phase two-level PWM inverter with a star connection load is shown in Fig. 1.

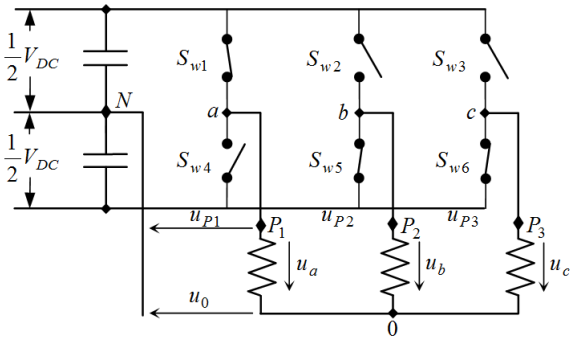

Fig.1: *Three phase two levels PWM inverter.*

In Fig. 1, u_{Pi}, $i = 1, 2, 3$, are pole voltages; u_a, u_b, and u_c are phase voltages; u_0 is neutral point voltage; V_{DC} is the DC link voltage of PWM. Their relationships are:

$$\begin{aligned} u_{Pi} &= \pm\frac{1}{2}V_{DC} \quad i = 1, 2, 3 \\ u_0 &= \pm\frac{1}{6}V_{DC} \\ u_a &= u_{P1} - u_0; u_b = u_{P2} - u_0; u_c = u_{p3} - u_0 \end{aligned} \quad (1)$$

The SVM principle is based on the switching between two adjacent active vectors and two zero vectors during one switching period [19]. From Fig. 1, the output voltages of the inverter can be composed by eight switch states $U_0, U_1, \cdots, U_7$, corresponding to the switch states $S_0(000)$, $S_1(100)$,..., $S_7(111)$, respectively. These vectors can be plotted on the complex plane (α, β) as shown in Fig. 2.

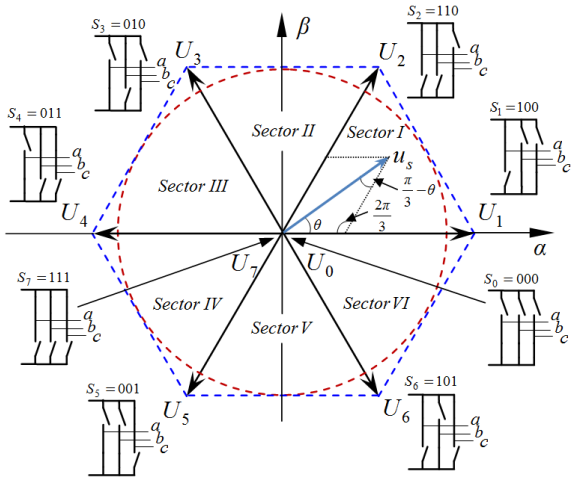

Fig.2: *Space vectors.*

The rotating voltage vector within the six sectors can be approximated by sampling the vector and switching between different inverter states during the sampling period. This will produce an approximation of the sampled rotating space vector. By continuously sampling the rotating vector and high frequency switching, the output of the inverter will be a series of pulses that have a dominant fundamental sine wave component, corresponding to the rotation frequency of the vector [20]. In order to reduce the number of switching actions and make full use of active turn-on time for space vectors, the vector u_s is commonly split into two nearest adjacent voltage vectors and zero vectors S_0 and S_7 in an arbitrary sector. For example, during one sampling interval, vector u_s in sector I can be expressed as

$$u_s(t) = \frac{T_0}{T_s}U_0 + \frac{T_1}{T_s}U_1 + \frac{T_2}{T_s}U_2 + \frac{T_7}{T_s}U_7 \quad (2)$$

where T_s is the sampling time, and $T_s - T_1 - T_2 = T_0 + T_7 \geq 0$, $T_0 \geq 0$ and $T_7 \geq 0$. The required time T_1 to spend in active state U_1 is given by the fraction of U_1 mapped by the decomposition of the required space vector u_s onto the U_1 axis, shown in Fig. 2 as U_{1X}. Therefore

$$T_1 = \frac{|U_{1X}|}{U_1}T_s \quad (3)$$

and similarly

$$T_2 = \frac{|U_{2X}|}{U_1}T_s \quad (4)$$

From Fig. 2, the amplitude of vector U_{1X} and U_{2X} are obtained in terms of $|u_s|$ and θ,

$$\frac{|u_s|}{\sin(\frac{2\pi}{3})} = \frac{|U_{2X}|}{\sin\theta} = \frac{|U_{1X}|}{\sin(\frac{\pi}{3}-\theta)} \quad (5)$$

Based on the above equations, the required time period spending in each of the active and zero states are given by

$$\begin{aligned} T_1 &= \frac{|u_s|\sin\left(\frac{\pi}{3}-\theta\right)}{|U_1|\sin\left(\frac{2\pi}{3}\right)}T_s, \quad T_2 = \frac{|u_s|\sin\left(\frac{\pi}{3}-\theta\right)}{|U_2|\sin\left(\frac{2\pi}{3}\right)}T_s \\ T_z &= T_0 + T_7 = T_s - (T_1 + T_2) \end{aligned} \quad (6)$$

The pulse command signals pattern for the inverter for Sector I can be constructed in Fig. 3. Similarly, according to the vector sequence and timing during a sampling interval given in Table 1, other five pulse command signal patterns, associated with sector II, sector III, ..., sector VI can be obtained.

Table 1: *Time duration for selected vectors.*

U_0	U_m^a	U_n^a	U_7	U_n	U_m	U_0
$\frac{T_z}{4}$	$\frac{T_m}{2}$	$\frac{T_n}{2}$	$\frac{T_z}{2}$	$\frac{T_n}{2}$	$\frac{T_m}{2}$	$\frac{T_z}{4}$

U_m and Un are two adjacent voltage vectors.

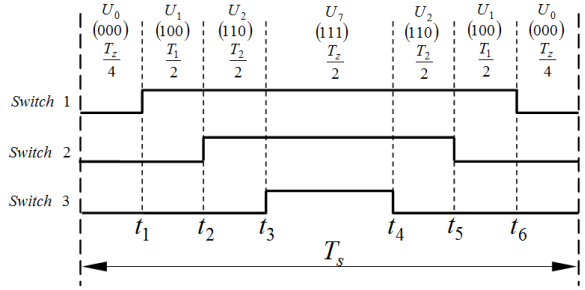

Fig.3: *Pulse command signal pattern.*

Hence the required time periods in a sampling interval can be given as

$$\begin{aligned} t_1 &= \frac{T_z}{4} \\ t_2 &= \begin{cases} \frac{T_z}{4} + \frac{T_m}{2}, & sector = I, III, V; \\ & m = 1,3,5, respactively \\ \frac{T_z}{4} + \frac{T_n}{2}, & sector = II, IV, VI; \\ & m = 3,5,1, respactively \end{cases} \\ t_3 &= \frac{T_z}{4} + \frac{T_m + T_n}{2} \\ t_4 &= \frac{3T_z}{4} + \frac{T_m + T_n}{2} \\ t_5 &= \begin{cases} \frac{3T_z}{4} + \frac{T_m}{2} + T_{m+1}, & sector = I, III, V; \\ & m = 1,3,5, respactively \\ \frac{3T_z}{4} + \frac{T_n}{2} + T_m, & sector = II, IV, VI; \\ & m = 2,4,6 and \\ & n = 3,5,1, respactively \end{cases} \\ t_6 &= \frac{3T_z}{4} + T_m + T_n \end{aligned} \quad (7)$$

3. SLIDING MODE CONTROLLER DESIGN

The objective of SMC design is to make the modulus of the rotor flux vector ψ_r , and torque T track to their reference value ψ_r^* and T^*, respectively.

3.1 Selection of the sliding surfaces

The transient dynamic response of the system is dependent on the selection of the sliding surfaces. The selection of the sliding surfaces is not unique. The higher-order sliding modes can be selected; however, it demands more information in implementation [21]. Considering the SMC design for an induction motor wheel drives supplied through an inverter (Fig. 1), two sliding surfaces are defined as

$$S_1 = T^* - \hat{T} \quad (8)$$

$$S_2 = C(\psi_r^* - \hat{\psi}_r) + (\dot{\psi}_r^* - \dot{\hat{\psi}}_r) \quad (9)$$

The positive constant C determines the convergent speed of rotor flux. T^* and ψ_r^* are the reference torque and reference rotor flux, respectively. $\hat{T}$ and $\hat{\psi}_r$ are the estimated torque and rotor flux, and $\hat{\psi}_r = \sqrt{\hat{\psi}_\alpha^2 + \hat{\psi}_\beta^2}$ where $\hat{\psi}_\alpha^2$ and $\hat{\psi}_\beta^2$ are the estimated rotor flux in α, β coordinate. Once the system is driven into sliding surfaces, the system behavior will be determined by $S_1 = 0$ and $S_2 = 0$ in Eqs. (8) and (9). The objective of control design is to force the system into sliding surfaces so that the torque and rotor flux signals will follow the respective reference signals.

3.2 Invariant transformation of sliding surfaces

In order to simplify the design process, the time derivative of sliding surfaces function S can be decoupled with respect to two phase stator voltage vectors $u = [u_\alpha, u_\beta]^T$. Projection of the systems motion in the subspaces S_1 and S_2 can be written as

$$\frac{dS}{dt} = F + Au \quad (10)$$

where $F = [f_1, f_2]^T$, $u = [u_\alpha, u_\beta]^T$, and $S = [S_1, S_2]^T$.

Functions f_1, f_2, and matrix A can be obtained as follows by differentiating structure switching function (8) and (9) and substituting corresponding relations from the mathematical model,

$$f_1 = \dot{T}^* + \frac{3P}{2}\left(\frac{1}{R_r}\dot{\hat{\psi}}_r \cdot \hat{\psi}_r + \sigma L_s \hat{\psi}_r^2\right) \cdot \hat{\omega} + \sigma\gamma\hat{T} \quad (11)$$

$$f_2 = C\dot{\psi}_r^* + \ddot{\psi}_r^* + \sigma R_s R_r \hat{\psi}_r - \frac{2}{3P} R_r \frac{\hat{T}}{\hat{\psi}_r}\hat{\omega} - \left(\frac{2}{3P}\right)^2 R_r^2 \frac{\hat{T}^2}{\hat{\psi}_r^3} + \left(\frac{2R_r}{L_r} - C\right)\dot{\hat{\psi}}_r \quad (12)$$

$$A = \begin{bmatrix} a_1\hat{\psi}_\beta & -a_1\hat{\psi}_\alpha \\ a_2\hat{\psi}_\alpha & -a_2\hat{\psi}_\beta \end{bmatrix} \quad (13)$$

where P is the number of pole pairs, R_r and R_s are rotor and stator resistances, L_r and L_s are rotor and stator inductances, and L_m is the mutual inductance, $\sigma = 1/\left(L_s L_r - L_m^2\right)$, $\gamma = L_s R_r + R_s L_r$, $a_1 = (3P/2)\sigma L_m$ and $a_2 = -(1/\hat{\psi}_r)\sigma R_r L_m$; $\hat{\omega}$ is the estimated rotor angle velocity.

From Eqs. (11) and (12), it is noted that functions f_1 and f_2 do not depend on either u_α or u_β. Therefore the transformed sliding surfaces, $q = [q_1, q_2]^T$, are introduced to simplify the design process and to construct the candidate Lyapunov function in the next subsection. Sliding surfaces q and S are related by an invariant transformation:

$$q = A^T S \quad (14)$$

3.3 Selection of the control law

The direct method of Lyapunov is used for the stability analysis. Considering the Lyapunov function candidate $v = 0.5 S^T S \geq 0$, its time derivative is

$$\dot{v} = S^T (F + Au) \quad (15)$$

Select the control law as

$$u_\alpha = -k_1 sign(q_1) - k_2 q1 \quad (16)$$
$$u_\beta = -k_1 sign(q_2) - k_2 q1 \quad (17)$$

where $sign(q) = \begin{cases} +1, q > 0 \\ -1, q < 0 \end{cases}$; and k_1, k_2 are positive constants.

From the time derivative of Lyapunov function (15), the following equation can be derived:

$$\dot{v} = S^T(F + Au) = (q_1 f_1^* - k_1|q_1| - k_2 q_1^2) + (q_2 f_2^* - k_1|q_2| - k_2 q_2^2) \quad (18)$$

where $[f_1^*, f_2^*] = (A^{-1}F)^T$.

From Equation (18), it is noted that if one chooses $k_1 + k_2|q_i| > \max(f_i^*)$, where i=1,2, the time derivative of Lyapunov function $\dot{v} < 0$. Thus the origin in the space q (and in the space S as well) is asymptotically stable, and the reaching condition of sliding surface is guaranteed. The torque $\hat{T}$ and rotor flux $\hat{\psi}_r$ will approach to the reference torque and reference rotor flux, respectively.

From Equations (16) and (17), it is observed that the control command u_α is used to force sliding mode occurring on the manifold $q_1 = 0$, while u_β is used to force sliding mode occurring on the manifold $q_2 = 0$. The sliding mode occurring on the manifold $q = 0$ is equivalent to its occurrence on the manifold $S = 0$ [7]. After the sliding mode arises on the intersection of both surfaces $S_1 = T^* - \hat{T} = 0$ and $S_2 = C(\psi_r^* - \hat{\psi}_r) + (\dot{\psi}_r^* - \dot{\hat{\psi}}_r) = 0$, then $\hat{T} = T^*$ and $\hat{\psi}_r = \psi_r^*$. Therefore a complete decoupled control of torque and flux is achieved.

The next step is designing the control inputs so that the state trajectories are driven and attracted toward the sliding surfaces S_1 and S_2 , and then remain sliding on it for all subsequent time. Let us consider the positive definite Lyapunov function L defined as follows:

$$L_i = \frac{1}{2} S_i^2 \qquad \text{for } i = 1, 2 \quad (19)$$

The time derivative $\dot{L}$ of L must be negative definite $\dot{L} < 0$ to ensure system stability and make the surface S attractive. Such condition leads to the following inequality:

$$\dot{L}_i = S_i \cdot \dot{S}_i < 0 \quad (20)$$

The torque control block diagrams of the IM for electric vehicles propulsion system are shown in Fig. 4 (SMC with SVM), Fig. 5 (PI with SVM).

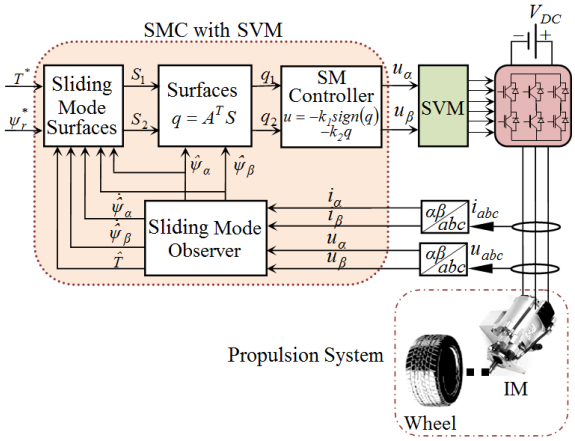

Fig.4: *The SMC with SVM of IM propulsion system.*

It is well known that sliding-mode techniques generate undesirable chattering and cause the torque, flux, and current ripple in the system. However, in the new control system, due to the SVM technique giving a large linear control range and the regular logic control signals for inverter [19], which means less harmonic distortion, the chattering can be effectively reduced.

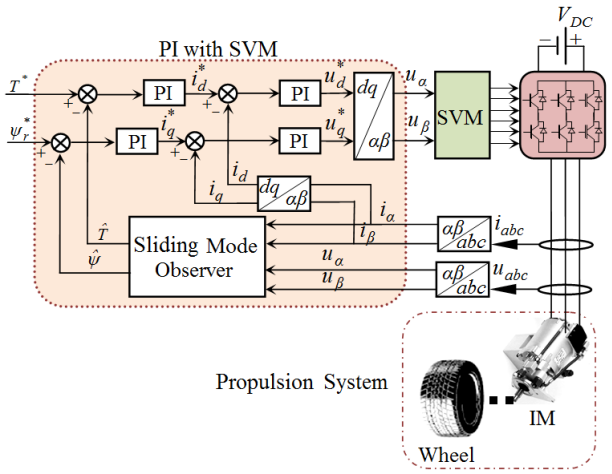

Fig.5: *The PI with SVM of IM propulsion system.*

4. SLIDING MODE FUZZY CONTROLLER DESIGN

The combination of SMC with the fuzzy logic control aims to improve the robustness and the performance of controlled nonlinear systems [9, 11, 12, 23]. The proposed sliding mode fuzzy control (SMFC) scheme for induction motors wheel drives torque control of the electric vehicle propulsion system is given in Fig. 6.

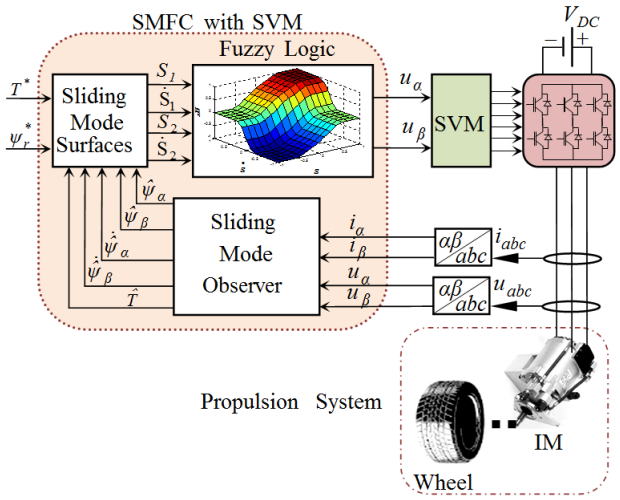

Fig.6: *The SMFC with SVM of IM propulsion system.*

Let us consider the sliding surfaces defined by Equations (8) and (9). The proposed sliding mode fuzzy controller forces the derivative of the Lyapunov function to be negative definite. Thus, the rule base table is established to satisfy Inequality (21).

Intuitively, suppose that $S_i > 0$ and $\dot{S}_i > 0$, the duty cycle must increase; if $S_i > 0$ and $\dot{S}_i > 0$, the duty cycle must decrease. Thus, the surfaces S_1 and S_2 whith its variation $\dot{S}_1$ and $\dot{S}_2$ are the inputs of the proposed controller. The outputs signals are the control increment $\overset{(k)}{\Delta U_\alpha}$ and $\overset{(k)}{\Delta U_\beta}$, which are used to update the control law. The control signals are defined as follows:

$$\overset{(k)}{\Delta U_\alpha} = \overset{(k)}{\Delta U_\alpha} + \overset{(k+1)}{U_\alpha} \tag{21}$$

$$\overset{(k)}{\Delta U_\beta} = \overset{(k)}{\Delta U_\beta} + \overset{(k+1)}{U_\beta} \tag{22}$$

The proposed sliding mode fuzzy controller is a zero-order Sugeno fuzzy logic controller, which is a special case of the Mamdani fuzzy inference system. Only the antecedent part of the Sugeno controller has the “fuzziness" and the consequent part is a crisp function. In the Sugeno fuzzy controller, the output is obtained through the weighted average of consequents [13, 14, 24].

Trapezoidal and triangular membership functions denoted by N (negative), Z (zero), and P (positive) are used for both the surface and surface changes. They are presented in Fig. 7 and Fig. 8 in the normalized domain. For the outputs signals, five normalized singletons denoted by NB (negative big), NM (negative middle), Z (zero), PM (positive middle), and PB (positive big) are used for the outputs signals (Fig. 9). The surface plot presentation relationship between the inputs and outputs parameters of the rule table given in Table 2 is visualized in Fig. 10.

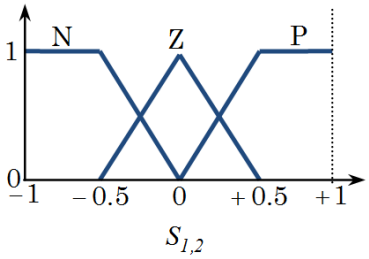

Fig.7: *Surfaces S_1 and S_2 membership functions.*

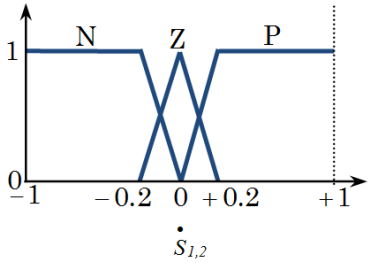

Fig.8: *Surfaces change $\dot{S}_1$ and $\dot{S}_2$ membership functions.*

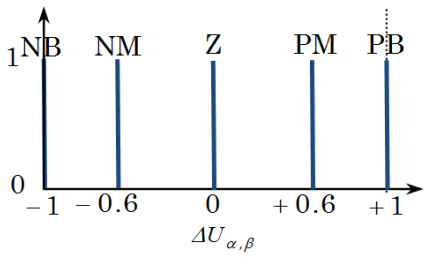

Fig.9: *Outputs singletons ΔU_α and ΔU_β membership functions.*

Table 2: *Proposed SMFC Rule Base.*

$\Delta U_{\alpha,\beta}$		$S_{1,2}$		
		P	Z	N
$\dot{S}_{1,2}$	P	PB	PM	Z
	Z	PM	Z	NM
	N	Z	NM	NB

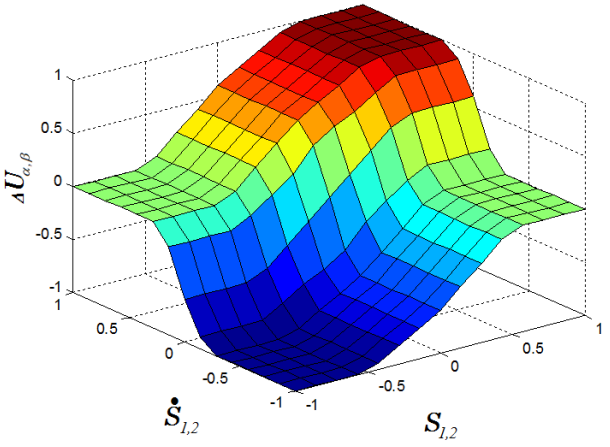

Fig.10: *Surfaces plot showing the relationship between the inputs and outputs parameters.*

5. SIMULATION RESULTS

In this section, simulation results are obtainable to show the performance of the proposed novel sliding mode fuzzy control method (SMFC with SVM). Meanwhile, the proposed control method has been compared with the conventional SMC [16] and classical PI control method [22]. The sliding-mode observer is adopted to estimate the rotor flux and the torque of an induction motor wheel drives of the electric vehicle propulsion system without using speed sensors [8]. This observer has been proved to have good convergence and asymptotic stability [16]. The block diagrams of torque control of the IM propulsion system are exposed in Fig. 4 (SMC with SVM), Fig. 5 PI with SVM.

In Fig. 4, u^*_α and u^*_β are control signals, derived from the control law (16) and (17), and in Fig. 2 $|u_s| = \sqrt{(u^*_\alpha)^2 + (u^*_\beta)^2}$, $\theta = atan(|u^*_\beta|/|u^*_\alpha|)$. In Fig. 5, the parameters of the PI controller are tuned by trial and error to achieve the best control performance. In Fig. 4, the inverter logic control signals are obtained through the SMC method while they are calculated by using SVM techniques, however in the proposed method (Fig. 6) the inverter logic control signals are obtained during the fuzzy logic controller associated with SMC though they are calculate by using SVM techniques. This turns out to be the major difference between the SMC alone with SVM and the proposed SMFC method with SVM.

To verify the technique proposed in this paper, digital simulations based on Matlab/Simulink have been implemented. The nominal parameters of the test induction motor of the electric vehicle propulsion system are listed in Table 3.

A Matlab S-function is developed to implement the SVM block. A 10-kHz fixed switching frequency for the inverter is used. For SMC with SVM, parameters k_1 and k_2 are selected as k_1=0.1 and k_2=0.3.

Table 3: *Type of Magnets.*

R_r	0.0503Ω
R_s	0.08233Ω
L_s	0.000724 H
L_m	0.02711 H
L_r	0.000724 H
P_N	35 KW
P	4

5.1 Simulation results of stator current, rotor torque and rotor flux

Figs. 11-13 show the stator current i_α, torque responses T, and rotor flux responses ψ_r when the reference torque signal is a rectangular wave with frequency 25 Hz. Based on the simulation results shown in Fig. 13, the output torque comparison of three control methods is shown in Table 4. From Fig. 11, it's noted that the resulting current has the largest harmonic distortion for PI with SVM, the smallest harmonic distortion for SMC with SVM, and negligible harmonic distortion for SMFC with SVM.

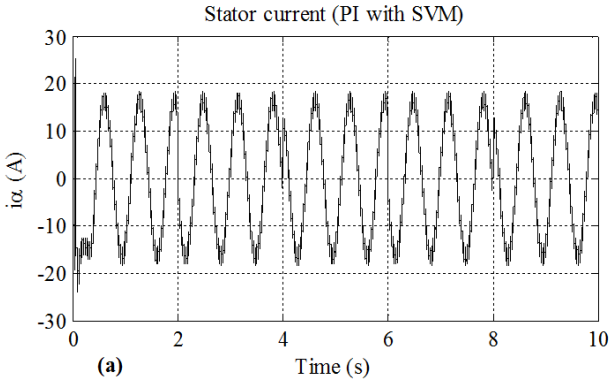

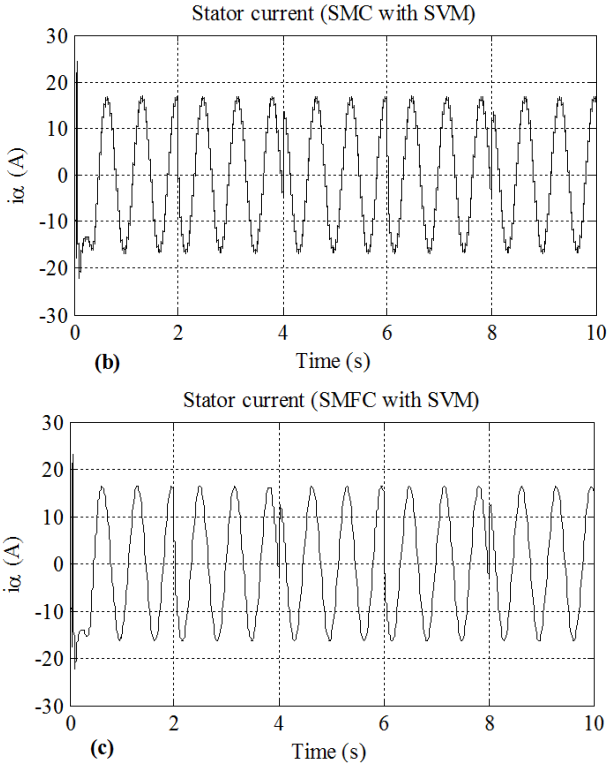

Fig.11: *Stator current i_α, (a) PI with SVM, (b) SMC with SVM, and (c) SMFC with SVM.*

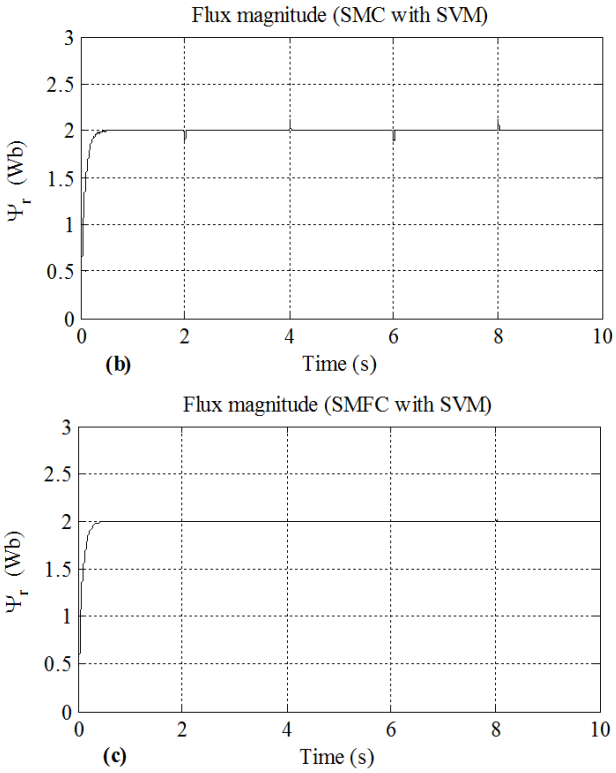

Fig.12: *Rotor flux responses ψ_r, (a) PI with SVM, (b) SMC with SVM, and (c) SMFC with SVM.*

Fig. 12 shows that the estimated rotor flux tracks the reference input well in all three control methods, but PI with the SVM control scheme has the most oscillation and biggest overshoot, while SMC with SVM has the least oscillations with no overshoot, and SMFC with SVM has no oscillations with no overshoot. Due to the rapid change of stator current, four disturbances appear at 2 s, 4 s, 6 s, and 8 s in Figs. 12(a) and 12(b). However, no disturbances are found in Fig. 12(c). This demonstrates the fact of the strong robustness of the sliding mode observer, and even the SMFC with SVM. Fig. 13 and Table 4 show that, among three control methods, SMFC with SVM has the best torque tracking performance with significant reduced torque ripple. The simulation results demonstrate that the new control approach can achieve the exact decoupling of the motor torque and rotor flux, and shows satisfactory dynamic performance.

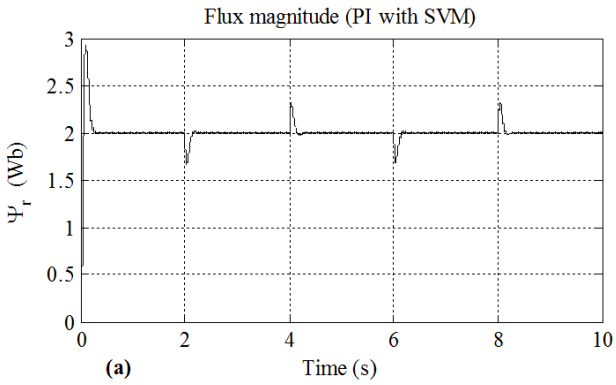

Table 4: *Type of Magnets.*

Controllers	Mean-square error of output torque	Torque ripple
PI with SVM	0.947%	±18.00%
SMC with SVM	0.266%	±6.235%
SMFC with SVM	0.005%	**±0.655%**

5.2 Torque tracking

In order to test the torque tracking convergence to various reference torque signals, different kinds of waves are selected as the reference torque signals. Figs. 14-16 show torque responses of the three control methods when the reference torque signals are sine wave, sawtooth wave and piecewise wave, respectively.

From Figs. 14-16, it is noted that the proposed new control method exhibits high accuracy in torque tracking when the reference torque signal is changed to different signals.

5.3 Load disturbances

To test the robustness of the developed sliding mode fuzzy control method, the external load dis-

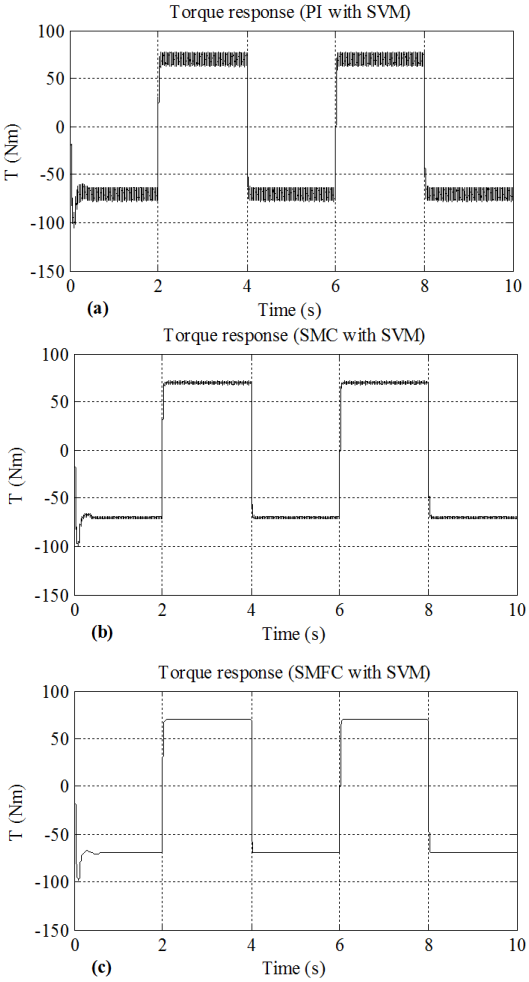

Fig.13: *Torque responses T, (a) PI with SVM, (b) SMC with SVM, and (c) SMFC with SVM.*

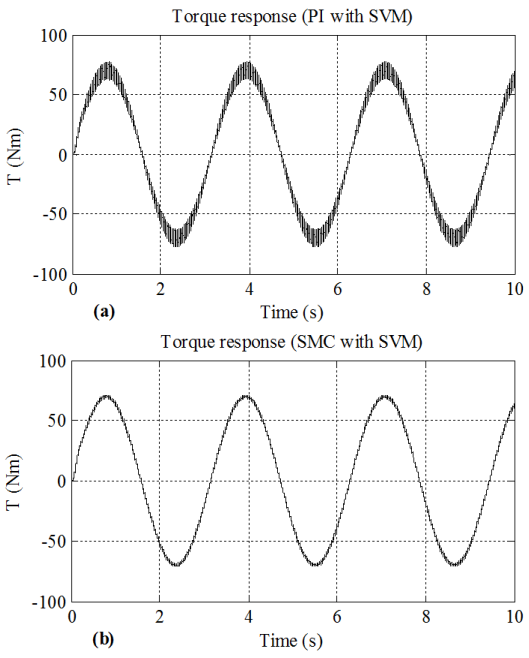

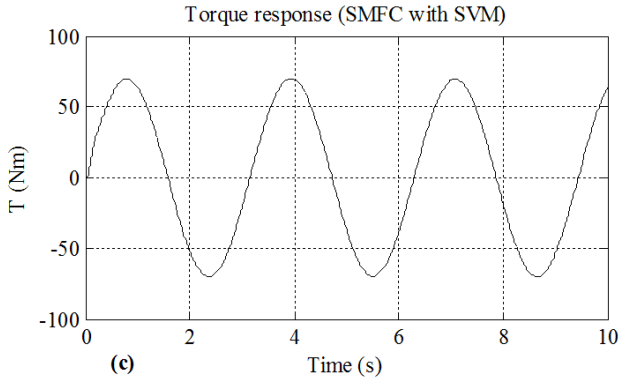

Fig.14: *Torque responses with a sine wave reference signal.*

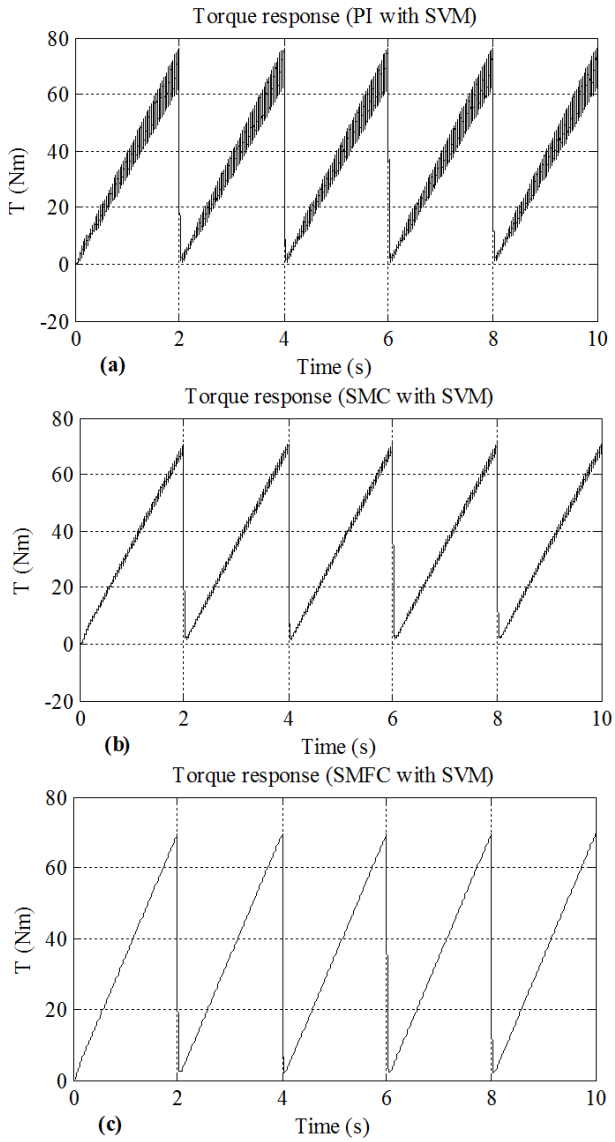

Fig.15: *Torque responses with a sawtooth reference signal.*

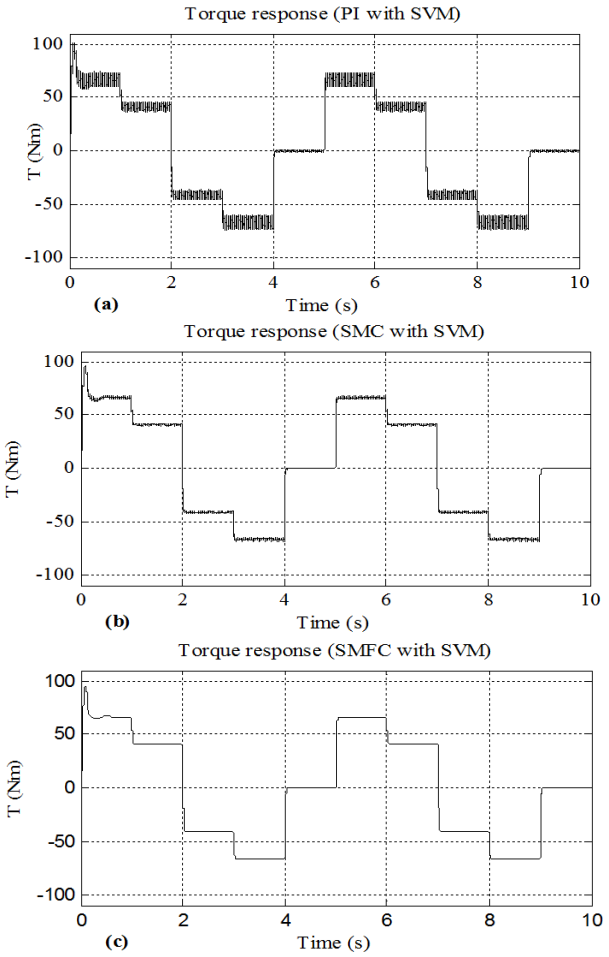

Fig.16: *Torque responses with a piecewise wave reference signal.*

turbance has been introduced to the proposed control system. Fig. 17 illustrates torque and speed responses of three control methods when external load disturbance is a bandlimited white noise with 6.25e-3 noise power.

From Fig. 17, it is demonstrated that the torque response of the proposed new control system is insensitive to external load perturbation. Although the speed has small oscillation because of the disturbance, the new control system is stable, and strong robust.

6. CONCLUSION

In this paper, a novel SMFC approach integrating with the SVM technique for an induction motor wheel drives of an electric vehicles propulsion system has been presented. Complete decoupled control of torque and flux is obtained and significant torque ripple reduction is achieved. Comparing with the classical PI control method, the conventional SMC method and SMFC with SVM technique, this new scheme has low torque ripple, low current distortion, and highperformance dynamic characteristics. Moreover, this new control scheme can achieve high accuracy

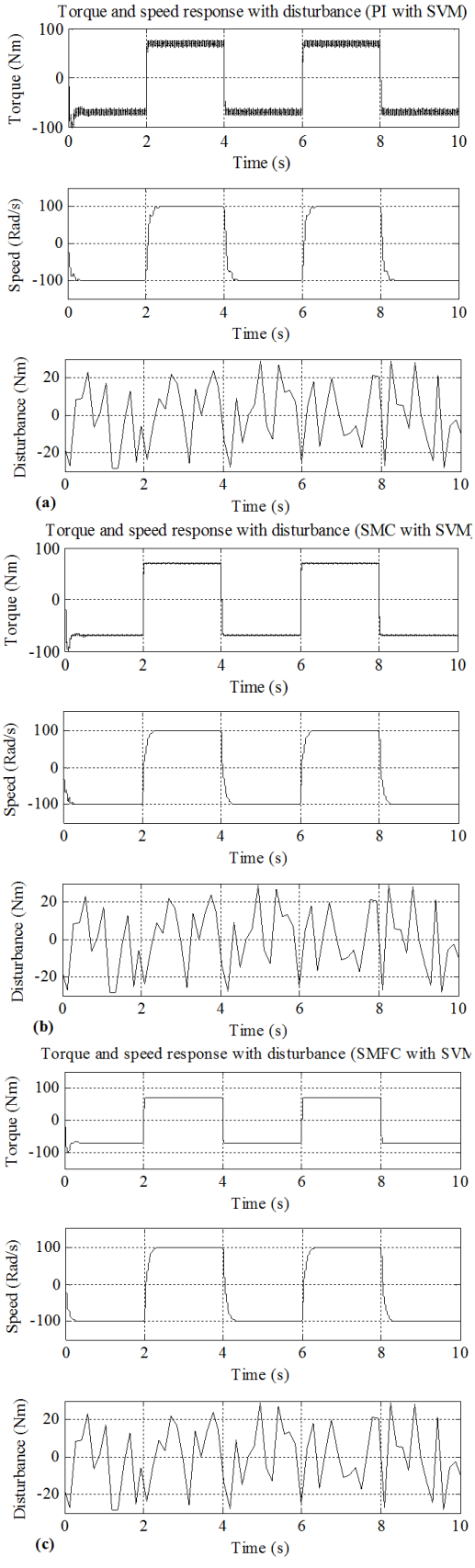

Fig.17: *Torque and speed responses with disturbance.*

in torque tracking to various reference torque signals and shows very strong robustness to external load disturbances. Therefore the proposed novel control method is simple, accurate, and robust. This study demonstrates the robustness and the dynamic performance of a new sliding mode fuzzy control scheme for torque control of induction motors of the electric vehicles propulsion system.

References

[1] C. C. Chan, "The state of the art of electric and hybrid vehicles," *Proceedings of the IEEE*, vol. 90, no. 2, pp. 247–275, 2002.

[2] C. A. Martins and A. S. Carvalho, "Technological trends in induction motor electrical drives," *IEEE Power Tech*, 2001.

[3] Tripathi, R. S. Anbarasu and R. Somakumar, "Control of ac motor drives: performance evaluation of industrial state of art and new techinique," *IEEE Int. Conf. Industrial Tech. (ICIT)*, pp. 3049–3054, 2006.

[4] M. Rodic and K. Jezernik, "Speed-sensorless sliding mode torque control of an induction motor," *IEEE Trans. Ind. Electron.*, vol. 49, pp. 87–95, 2002.

[5] F. Chen and M. W. Dunnigan, "Sliding-mode torque and flux control of an induction machine," *IEE Proc.: Electr. Power Appl.*, vol. 150, pp. 227–236, 2003.

[6] F. Barrero, A. Gonzalez, A. Torralba, E. Galvan and L. G. Franquelo, "Speed control of induction motors using a novel fuzzy sliding-mode structure," *IEEE Trans. Fuzzy Syst.*, vol. 10, pp. 375–383, 2002.

[7] V. I. Utkin, "Sliding Modes in Control and Optimization," *Springer-Verlag*, Berlin, 1992.

[8] V. I. Utkin, "Sliding mode control design principles and applications to electric drives," *IEEE Trans. Ind. Electron.*, vol. 40, pp. 23–36, 1993.

[9] F. Song and S. M. Smith, "A comparison of sliding mode controller and fuzzy sliding mode controller," *NAFIPS'2000, The 19th Int. Conference of the North American Fuzzy Information Processing Society*, pp. 480–484, 2000.

[10] S. B. Choi, C. C. Cheong and D. W. Park, "Moving switching surfaces for robust control of second order variable structure systems," *Int. J. of Control*, vol. 58, no. 1, pp. 229–245, 1993.

[11] Q. P. Ha, D.C. Rye and H.F. Durrant-Whyte, "Fuzzy moving sliding mode control with application to robotic manipulators," *Automatica*, vol. 35, pp. 607–616, 1999.

[12] H. Lee, E. Kim, H. Kang and M. Park, "Design of sliding mode controller with fuzzy sliding surfaces," *IEE Proc. Control Theory and Applications*, vol. 145, no. 5, 1998.

[13] H. Temeltas, "A fuzzy adaptation technique for sliding mode controllers," *Proc. IEEE Int. Symposium on Intelligent Control*, Columbus, Ohio, USA, pp. 15–18, 1994.

[14] S. W. Kim and J. J. Lee, "Design of a fuzzy controller with fuzzy sliding surface," *Fuzzy Sets and Systems*, vol. 71, pp. 359–367, 1995.

[15] R. Soto and K. S. Yeung, "Sliding-mode control of induction motor without flux measurement," *IEEE Trans. Ind. Appl.*, vol. 31, pp. 744–750, 1995.

[16] Z. Yan, C. Jin, and V. I. Utkin, "Sensorless sliding-mode control of induction motors," *IEEE Trans. Ind. Electron.*, vol. 47, pp. 1286–1297, 2000.

[17] A. Benchaib, A. Rachid, and E. Audrezet, "Real-time sliding-mode observer and control of an induction motor," *IEEE Trans. Ind. Electron.*, vol. 46, pp. 128–137, 1999.

[18] C. Lascu, and A. M. Trzynadlowski, "Combining the principles of sliding mode, direct torque control, and space-vector modulation in a high-performance sensorless AC drive," *IEEE Trans. Ind. Appl.*, vol. 40, pp. 170–176, 2004.

[19] J. Holtz, "Pulse width modulation for electronic power conversion," *IEEE Proc.*, vol. 82, pp. 1194–1213, 1994.

[20] K. Zhou and D. Wang, "Relationship between space vector modulation and three-phase carrier-based PWM: A comprehensive analysis," *IEEE Trans. Ind. Electron.*, vol. 49, pp. 186–196, 2002.

[21] W. Perruquetti, "Sliding Mode Control in Engineering," *Marcel Dekker*, Inc., New York, 2002.

[22] M. Tursini, R. Petrella and F. Parasiliti, "Adaptive sliding-mode observer for speed-sensorless control of induction motors," *IEEE Trans. Ind. Appl.*, vol. 36, pp. 1380–1387, 2000.

[23] A. Nasri, A. Hazzab, I. K. Bousserhane, S. Hadjeri and P. Sicard, "Fuzzy-Sliding Mode Speed Control for Two Wheels Electric Vehicle Drive," *Journal of Electrical Engineering & Technology*, Vol. 4, no. 4, pp. 499–509, 2009.

[24] 24_28 M. K. Passino, "Fuzzy control," *Addison-Wesley*, London, 2000.

Boumediène Allaoua received his diploma in Electrical Engineering from Bechar University, Algeria. He took his master's degree from the same university and his PhD from the Faculty of Sciences and Technology, Bechar University. Currently, he teaches electrical engineering at Bechar University. His research interests include power electronics robust control for electric vehicles and propulsion systems, power electronics development, electric drives robust control, modern control techniques, and artificial intelligence and its applications.

Abdellah Laoufi received his state engineer degree in Electrical Engineering from the University of Sciences and Technology of Oran (USTO), Algeria. He took his MSc and PhD from the Electrical Engineering Institute of the University of Djillali Liabes, Algeria. He is currently a professor of electrical engineering at Bechar University. His research interests include power electronics, electric drives control, and electric vehicle propulsion system control and its applications.